J Incl Phenom Macrocycl Chem (2010) 67:451–460
DOI 10.1007/s10847-009-9728-1

ORIGINAL ARTICLE

Complexation of metal ions with double-armed diazadithia lariat ether carrying anthracene moieties in acetonitrile–dioxane

Semanur Parlayan · Aysel Başoğlu · Yasemin Göbel · Miraç Ocak · Hakan Alp · Halit Kantekin · Ümmühan Ocak

Received: 25 June 2009 / Accepted: 10 December 2009 / Published online: 7 January 2010
© Springer Science+Business Media B.V. 2010

Abstract A new 14-membered crown ether with nitrogen–sulfur donor atom carrying two anthryl groups was designed and synthesized by the reaction of the corresponding macrocyclic compound and 9-(chloromethyl) anthracene. The influence of metal cations such as Al^{3+}, Zn^{2+}, Fe^{2+}, Fe^{3+}, Co^{2+}, Ni^{2+}, Mn^{2+}, Cu^{2+}, Cd^{2+}, Hg^{2+} and Pb^{2+} on the spectroscopic properties of the ligand was investigated in acetonitrile–dioxane solution (1/1) by means of absorption and emission spectrometry. The results of spectrophotometric titration experiments disclosed the complexation stoichiometry and complex stability constant of the novel ligand with Fe^{2+}, Fe^{3+}, Al^{3+}, Cd^{2+}, Cu^{2+}, Zn^{2+}, Pb^{2+} and Hg^{2+} cations. Absorption spectra show isobestic points in the spectrophotometric titration of these cations. The presence of excess of Al^{3+}, Zn^{2+}, Fe^{2+}, Fe^{3+}, Co^{2+}, Ni^{2+}, Mn^{2+}, Cu^{2+}, Cd^{2+}, Hg^{2+} and Pb^{2+} cations caused an enhancement of anthryl fluorescence. Especially, the enhancement in case of the interaction of Hg^{2+} and Al^{3+} cations with the ligand was pronounced.

S. Parlayan · Y. Göbel · M. Ocak · H. Kantekin · Ü. Ocak (✉)
Department of Chemistry, Faculty of Arts and Sciences, Karadeniz Technical University, 61080 Trabzon, Turkey
e-mail: ummuhanocak@yahoo.com

H. Alp
Karadeniz Technical University, Maçka Vocational School, Maçka, Trabzon, Turkey

A. Başoğlu
Bayburt University, Bayburt Vocational School, Bayburt, Turkey

Keywords Crown ether · 9-(chloromethyl) anthracene · Fluorescence spectroscopy · Stability constant · Metal cation

Introduction

Fluorescent cation sensors are of great interest because of their selective and sensitive cation determination properties [1–5]. Molecular systems that consist of a recognition part (ionophore) and a signaling part (fluorophore) have been used for this aim. A molecular cation sensor has to bind desired cation selectively between other cations. On the other hand, the signaling part is important for sensitivity of the sensor.

The fluorescent cation sensors having a simple spacer such as a methylene group, connecting the binding part and the signaling part, have been commonly employed [6–9]. Crown ethers have been used as cation binders in such molecular systems. "Fluorophore-spacer-receptor" systems have many advantages in monitoring the interaction of cation–macrocyclic. Upon cation binding, the fluorescence intensity of the fluorophore group may increase or decrease. Such photo-physical changes have been explained with photoinduced charge transfer (PCT), photoinduced electron transfer (PET) or excimer or exciplex emission [10]. Recently, PET has been explored extensively in the presence of metal cations in solution [11–13]. These investigations brought out effective cation sensors.

Anthracene and its derivatives have been used as signaling groups in the design of fluorescent cation chemosensors [14–16]. These groups have shown very interesting photo-physical properties. Some sensor systems carrying anthryl-aza crown ether were developed to show the cation complexation in the crown cavity. Upon complexation the

chelation enhanced fluorescence (CHEF) or chelation enhanced quenching (CHEQ) was observed for these systems [17–20].

In the present study we report the preparation of a 14-membered diazadithia crown ether ligand having two anthryl sidearms, **(3)**, and present the complexation properties of the ligand with a series of metal cations. Stability constant is an important parameter to disclose the effectiveness of the ligand in cation binding. Therefore we calculated the complex stability constants and complex compositions of metal cations with the ligand by using spectrophotometric titrations in acetonitrile–dioxane solution (1/1). We propose the new fluorescent ligand for aluminium determination.

Experimental

Chemicals

Acetonitrile and 1,4-dioxane from Merck (spectrometric grade) were the solvents for absorption and fluorescence measurements. All metal perchlorates purchased from Acros were of the highest quality available and vacuum dried over blue silicagel before use.

Apparatus

^{1}H NMR spectra were recorded on a Varian 200 A spectrometer, using $CDCl_3$ with TMS as the internal reference. IR spectra were recorded on a Perkin-Elmer 1600 FTlR spectrophotometer using KBr pellets. Elemental analysis was performed on Costech 4010 CHNS instrument. The absorption spectra of the solutions were recorded using a Thermo Evolution 60 model spectrophotometer. A Photon Technologies International Quanta Master Spectrofluorimeter (model QM-4/2006) was used for all fluorescence measurements.

Measurements

Absorption spectra of ligand **(3)** with a concentration of 2.58×10^{-5} M in acetonitrile–dioxane solution (1/1) containing 10 M equivalents of appropriate metal perchlorate salt were measured using 1-cm long absorption cell. Fluorescence spectra of the ligand solutions of 2.58×10^{-6} M were measured in 1-cm quartz cell. Excitation wavelength was 368 nm for **(3)**. Fluorescence emission spectra were recorded in the range 380–500 nm with slit width 1.0 nm.

The stoichiometry of the complexes was determined by using the molar-ratio method. The stability constants were calculated according to the previously described procedure [21].

Synthesis of the ligand **(3)**

Compound **(1)** [22] (0.44 g, 1.32 mmol) was dissolved in tetrahydrofuran (15 mL) and purged under nitrogen atmosphere in a Schlenk system connected to a vacuum line. A solution of 9-(chloromethyl) anthracene **(2)** (0.60 g, 2.64 mmol) in tetrahydrofuran (15 mL) was added dropwise to this solution for 30 min at 40 °C. Triethylamine (0.85 g, 8.41 mmol) was added to the mixture at this temparature. The reaction mixture was refluxed and stirred at reflux temperature for 48 h, monitored by TLC [silica gel, dichloromethane:ethyl alcohol (17:1)]. At the end of this period, the reaction mixture was filtered. The filtrate was concentrated on an evaporator to 10 mL and the solid formed was filtered off, washed with cold diethyl ether, then dried in vacuo. The pale yellow solid product (yield 89.0%) was obtained by recrystallization from benzene, mp 274–276 °C. Anal. Calc.for $C_{48}H_{42}N_2S_2$: C, 81.09; H, 5.95; N, 3.94; S, 9.02%. Found: C, 81.28; H, 5.83; N, 3.96; S, 8.91%. IR (KBr pellets, cm^{-1}): 3085 (Ar–H), 2898–2833 (C–H), ^{1}H-NMR ($CDCl_3$) : (δ) 6.92–7.26 (m, 8H, macrocyclic Ar–H), 7.35–8.59 (m, 18H, anthracene Ar–H) 4.70 (s, 4H, anthracene –CH_2), 3.77 (s, 4H, benzen–CH_2), 2.79–3.77 (m, 8H, N–CH_2 and S–CH_2), ^{13}C-NMR ($CDCl_3$): (δ) 134.41, 131.67, 129.36, 128.59, 127.97, 127.59, 125.93, 125.36, 125.11, 55.43, 54.32, 47.16, 33.93.

Results and discussion

Characterization of the ligand **(3)**

The synthetic pathway to the new ligand **(3)** is summarized in Scheme 1.

Compound **(3)** was synthesized by the reaction of compound **(1)** with 9-(chloromethyl) anthracene **(2)** in THF. The absence of the secondary amine band belonging to the starting material **(1)** in the IR spectra of the crown ether **(3)** with anthryl side arms has supported the structure. In the ^{1}H-NMR spectrum of **(3)**, the singlets (4H each) belong to the methylene protons of anthryl groups and benzylic methylene protons are observed at $\delta = 4.70$ ppm and $\delta = 3.77$ ppm, respectively. The multiplet (8H) between $\delta = 2.79$ ppm and $\delta = 3.77$ ppm belongs to N–CH_2 and S–CH_2 protons. Elemental analysis results confirm the proposed structure.

Absorption spectra

The absorption spectra of the ligand **(3)** in acetonitrile–dioxane (1/1) display the strong π–π^* absorption bands at 330–400 nm characteristic of the pendant anthracenyl groups [23]. As seen from Fig. 1, the ligand **(3)** possesses

Scheme 1 Synthetic pathway to the new crown ether, i.e. the ligand **(3)** used in this study

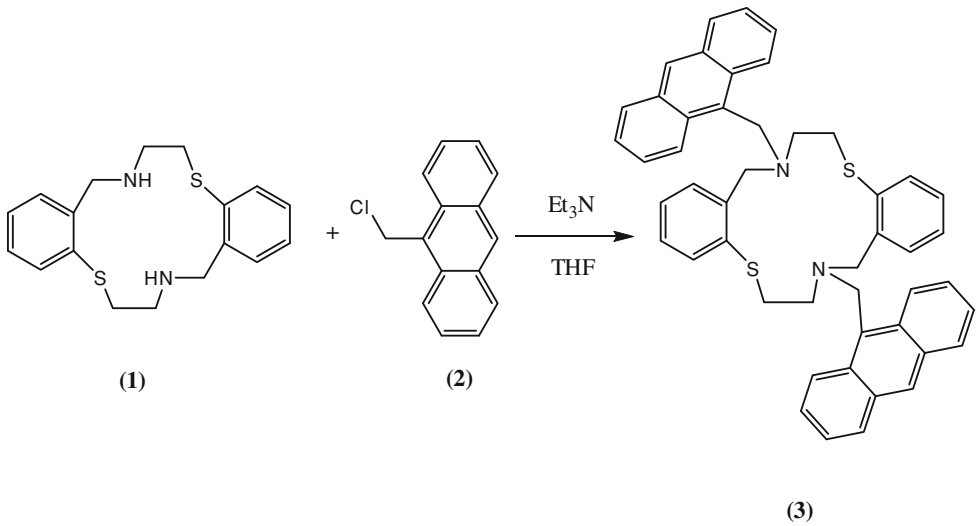

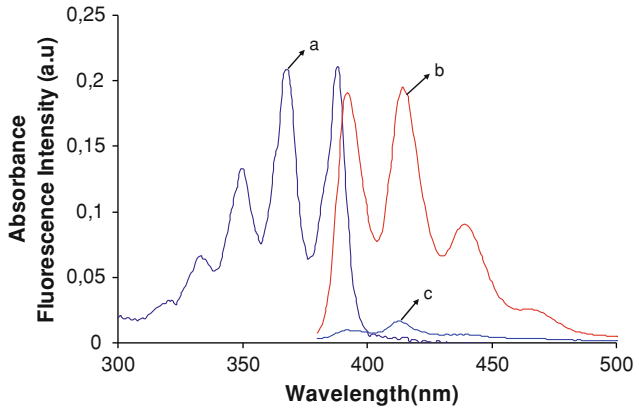

Fig. 1 UV absorption (**a**) and emission spectra (**c**) of the ligand **(3)** in acetonitrile–dioxane solution (1/1). Ligand concentrations are 2.58×10^{-5} M and 2.58×10^{-6} M for absorption and emission spectra, respectively. Excitation wavelength is 368 nm. **b** shows the fluorescence spectra of 1.93×10^{-6} M 9-(chloromethyl) anthracene in acetonitrile–dioxane solution (1/1)

four absorption bands at 334, 350, 368 and 388 nm. Molar absorption coefficients are, 4.7×10^3, 1.0×10^4, 1.6×10^4 and 1.6×10^4 cm^{-1} M^{-1} in these wavelengths, respectively.

Figure 2 shows the effect of metal cations on the absorption spectra of the ligand **(3)**. The presence of 10 equivalents of Cu^{2+}, Hg^{2+}, Al^{3+}, Fe^{2+}, Pb^{2+} and Fe^{3+} ions caused significant changes on the absorption spectra of the ligand (Fig. 2a) where red shifts at the absorption bands were observed. These red shifts were about 5 nm for Cu^{2+}, Hg^{2+}, Al^{3+}, Fe^{2+} and Fe^{3+} ions. There was only a red shift by 2 nm in the case of Pb^{2+}. On the other hand, absorption decreases were observed for Cu^{2+}, Hg^{2+}, Al^{3+}, Fe^{2+} and Pb^{2+} at the 368 and 388 nm absorption bands. The effects of Fe^{3+} is different from the other metal cations, i.e. Fe^{3+} caused absorption enhancements at the 350 and 368 nm absorption bands. However, this cation decreased the absorption at 388 nm with a red shift by 6 nm. Figure 2b shows the effect of Cd^{2+}, Co^{2+}, Ni^{2+}, Mn^{2+} and Zn^{2+} cations on the absorption spectra of the ligand. The presence of 10 equivalents of Cd^{2+}, Co^{2+} and Mn^{2+} cations produced modest changes in the absorption of the ligand where absorption decreases at 368 and 388 nm were observed. Ni^{2+} and Zn^{2+} caused very little red shift on these wavelengths. The absorption decreases were significant for both cations with respect to the others. As seen from Fig. 2b, the interaction of Ni^{2+} and Zn^{2+} with the ligand is approximately similar.

Spectrophotometric titrations

A regular change was observed in the absorption spectra of the ligand **(3)** with increasing concentrations of Fe^{2+}, Fe^{3+}, Al^{3+}, Cd^{2+}, Cu^{2+}, Zn^{2+}, Pb^{2+} and Hg^{2+} cations. Therefore the complex compositions and the complex stability constants for these cations were disclosed (Table 1). It is interesting that the effect of excess of these cations on the absorption spectra of the ligand **(3)** is similar except for Cd^{2+}. As seen from Fig. 2a, the shape of the absorption spectra changed for these cations. The broad bands on the spectra were seen in case of the mentioned cations. However, the absorption maximums of the ligand spectra were valid in the presence of Cd^{2+} (Fig. 2b). We couldn't find a regular change in the absorption spectra of the ligand **(3)** with increasing concentrations of Ni^{2+}, Mn^{2+} and Co^{2+} cations. It is interesting that the effect of excess of these cations on the absorption spectra of the ligand **(3)** is also similar. As seen from Fig. 2b, the presence of 10 equivalents of these cations produces only modest decreases in the absorption of 368 and 388 nm.

The change in the absorption spectra of the ligand **(3)** with increasing concentrations of Cu^{2+} is shown in Fig. 3. There were three isobestic points at 374, 380 and 394 nm.

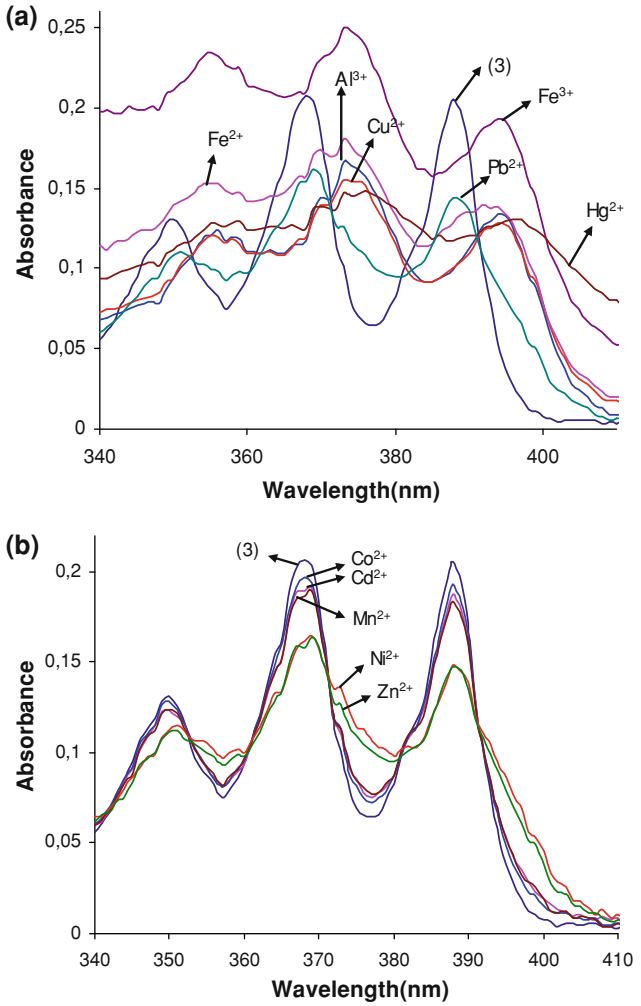

Fig. 2 The effect of metal cations on the absorption spectra of the ligand **(3)** in acetonitrile–dioxane solution (1/1). Ligand concentration = 2.58×10^{-5} M. Metal perchlorate concentrations = 2.58×10^{-4} M. **a** For Al^{3+}, Fe^{2+}, Fe^{3+}, Cu^{2+}, Hg^{2+} and Pb^{2+}. **b** For Zn^{2+}, Co^{2+}, Ni^{2+}, Mn^{2+}, Cd^{2+}

The isobestic point at 394 nm is well-pronounced. Other isobestic points were not clear when it was observed in detail. This seems to be due to the presence of small amounts of the free ligand and also due to a protonation equilibrium related to the ligand. On the other hand, the presence of many isobestic points indicates that there were more equilibriums than one during the complexation. The decrease of absorbance at 388 nm provided the determination of the complex composition of Cu^{2+}-ligand **(3)**. As seen from Fig. 3 (inset above), the inflection point was 2.0 ([M]/[L]). It can thus be concluded that the ligand **(3)** formed a stable 2:1 (M:L) complex with Cu^{2+}. In order to determine the complex stability constant, the ratio of $A_o/(A_o - A)$ was plotted against $[M]^{-1}$, as in Fig. 3 (inset below), which gave a good straight line. We obtained similar graphs for Fe^{2+}, Fe^{3+}, Al^{3+}, Cd^{2+}, Zn^{2+}, Pb^{2+} and Hg^{2+} cations. A_o and A are the absorbance of free ligand and the absorbance of the solution involving metal cation, respectively. The stability constant was calculated from the ratio intercept/slope [21]. The value of log K was 4.32 for the Cu^{2+}-complex (Table 1).

Table 1 Complex stability constants and complex composition of ligand **(3)** with metal cations in acetonitrile–dioxane (1:1) obtained by spectrophotometric titrations

Cation	Complex composition[a] (M:L)	Stability constant[a] (Log K)
Hg^{2+}	2:1	4.59 ± 0.14
Fe^{2+}	2:1	4.18 ± 0.12
Fe^{3+}	2:1	4.51 ± 0.09
Cu^{2+}	2:1	4.32 ± 0.02
Cd^{2+}	2:1	4.79 ± 0.56
Zn^{2+}	1:1	4.71 ± 0.09
Pb^{2+}	1:1	4.39 ± 0.20
Al^{3+}	1:1	4.75 ± 0.29

[a] Averages calculated from the data obtained from six independent absorbance measurements

Figure 4 shows the change in the absorption spectra of the ligand **(3)** with increasing concentrations of Cd^{2+}. The changes in the absorption spectra were very different from those in the case of other metal cations. There were little regular absorbance decreases at 368 and 388 nm. We disclosed the complex composition of Cd^{2+} from these absorption decreases at 388 nm. Figure 4 (inset above) shows the molar ratio plot for this complex. The inflection point was 2.0 ([M]/[L]). Therefore, we disclosed formation of a stable 2:1 (M:L) complex with Cd^{2+} from the absorbance changes at 388 nm. Figure 4 (inset below) shows the plot for the calculation of the stability constant of this complex. The value of log K was 4.79 for Cd^{2+}-complex. As seen from Fig. 4, the isobestic point at 382 nm is not clear because of the mentioned little absorbance changes in the spectra.

We also disclosed the 2:1 (M:L) complex for Fe^{2+}, Fe^{3+} and Hg^{2+} cations (Figs. 5, 6, 7). The regular decreases in the absorption spectra of the ligand **(3)** with increasing concentrations of Fe^{2+} were observed (Fig. 5) and a log K value of 4.18 was found for this complex (Fig. 5, inset below). However, the isobestic points were not clear. The effect of Fe^{3+} on the absorption spectra of the ligand **(3)** was different from that in the case of Fe^{2+} ion. There were red shifts with increasing concentrations of Fe^{3+} and as seen from Fig. 6, these red shifts were pronounced after [M]/[L] = 1.0. There were five isobestic points at 353, 361, 371, 381 and 391 nm indicating the presence of several equilibriums in the solution. The complex composition was 2:1 (M:L) for Fe^{3+} (see the inset above (break point is 2.0)). The value of log K was 4.51 in the case of the Fe^{3+}-complex (Table 1).

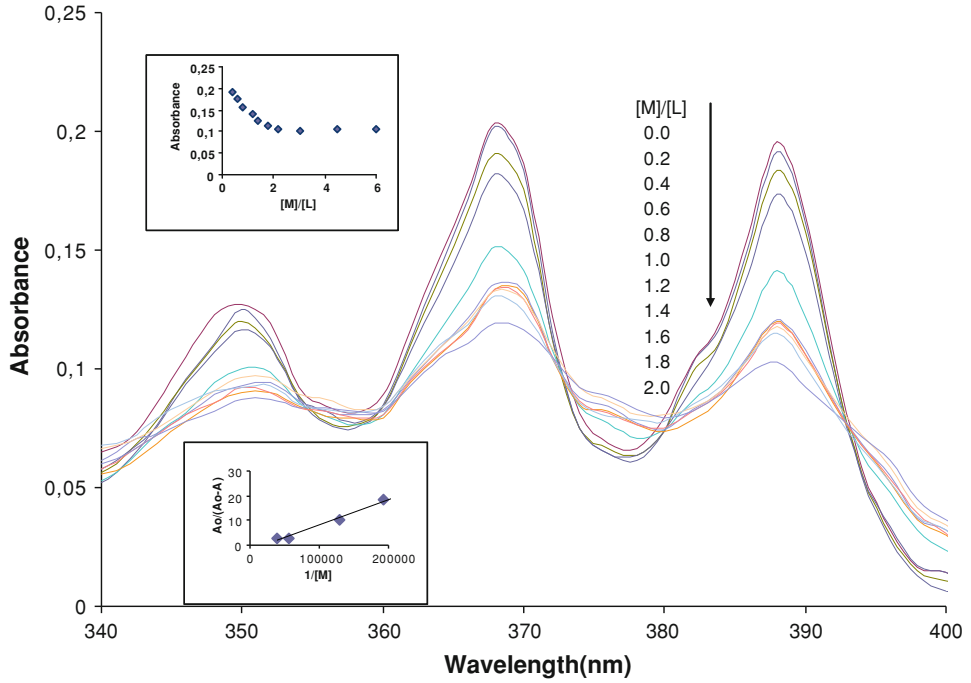

Fig. 3 The variation of the absorbance of the ligand **(3)** with the concentration of Cu^{2+}, added as 0–2 equivalents of $Cu(ClO_4)_2$. Ligand concentration = 2.58×10^{-5} M. *Insets*: Measurements were carried out at 388 nm

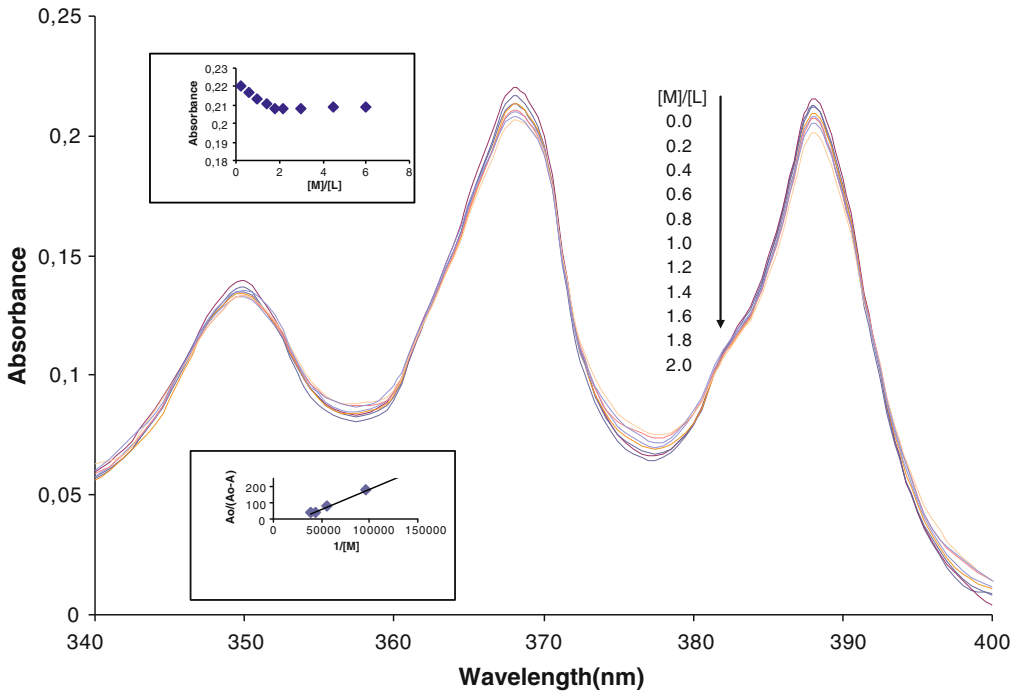

Fig. 4 The variation of the absorbance of the ligand **(3)** with the concentration of Cd^{2+}, added as 0–2 equivalents of $Cd(ClO_4)_2$. Ligand concentration = 2.58×10^{-5} M. *Insets*: Measurements were carried out at 388 nm

Figure 7 shows the change in the absorption spectra of the ligand **(3)** with increasing concentrations of Hg^{2+}. There were three isobestic points at about 354, 372, and 392 nm. However, the isobestic points were not clear. We disclosed the formation of a stable 2:1 (M:L) complex with Hg^{2+} from the absorbance changes at 388 nm. Figure 7 (inset above) shows the molar ratio plot for Hg^{2+} where the inflection point was 2.0 ([M]/[L]). It can thus be concluded

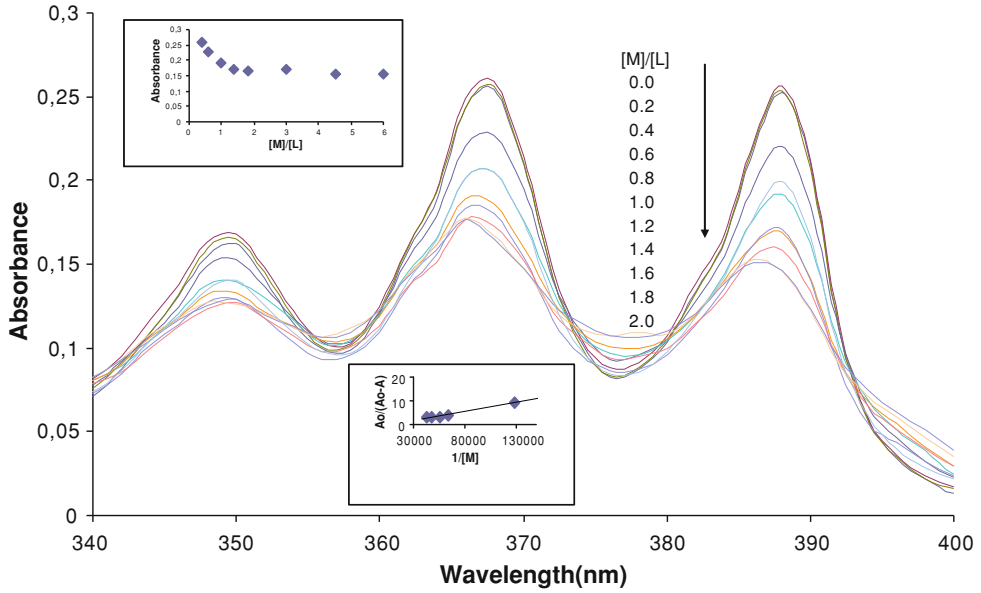

Fig. 5 The variation of the absorbance of the ligand **(3)** with the concentration of Fe^{2+}, added as 0–2 equivalents of $Fe(ClO_4)_2$. Ligand concentration = 2.58×10^{-5} M. *Insets*: Measurements were carried out at 388 nm

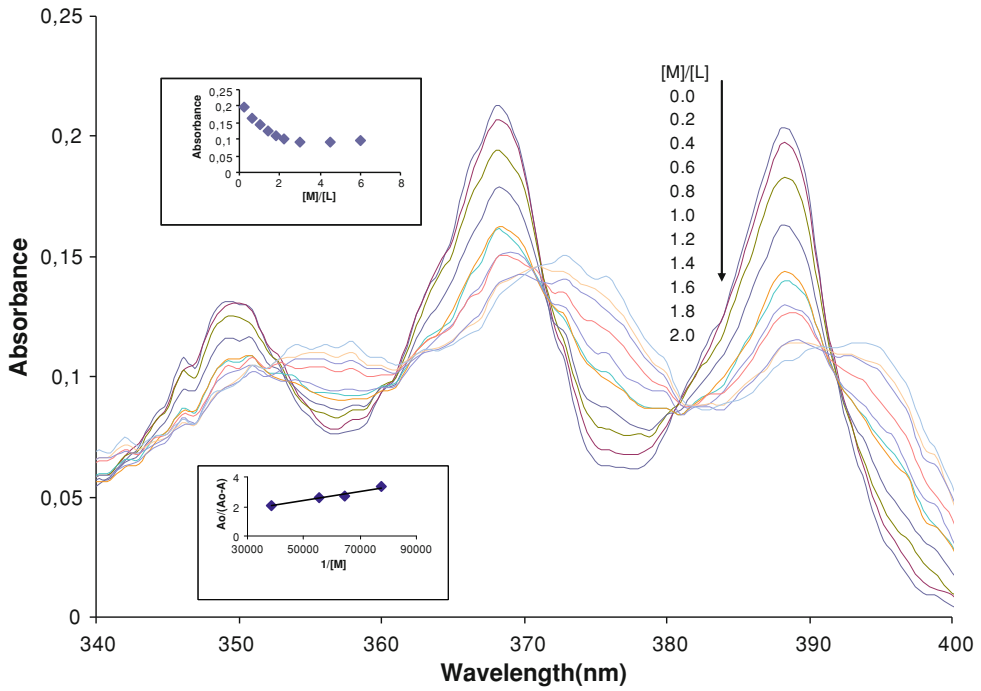

Fig. 6 The variation of the absorbance of the ligand **(3)** with the concentration of Fe^{3+}, added as 0–2 equivalents of $Fe(ClO_4)_3$. Ligand concentration = 2.58×10^{-5} M. *Insets*: Measurements were carried out at 388 nm

that the ligand **(3)** formed a stable 2:1 (M:L) complex with Hg^{2+}. The plot showing the ratio of $A_o/(A_o - A)$ versus $[M]^{-1}$ gave a good straight line and a log K value of 4.59 was calculated for the Hg^{2+}-complex (Table 1).

The change in the absorption spectra of the ligand **(3)** with increasing concentrations of Zn^{2+}, Pb^{2+} and Al^{3+} is shown in Figs. 8, 9, 10. These cations form 1:1 (M:L) complex with the ligand **(3)**. The effect of Zn^{2+} and Pb^{2+} on the absorption spectra is similar (Figs. 8, 9). There were five isobestic points at about 354, 362, 372, 382 and 394 nm for the both cations. This result indicates the presence of several equilibriums in the solution for these cations. On the other hand, a slight red shift was observed at 368 nm absorption band with increasing Zn^{2+} and Pb^{2+}

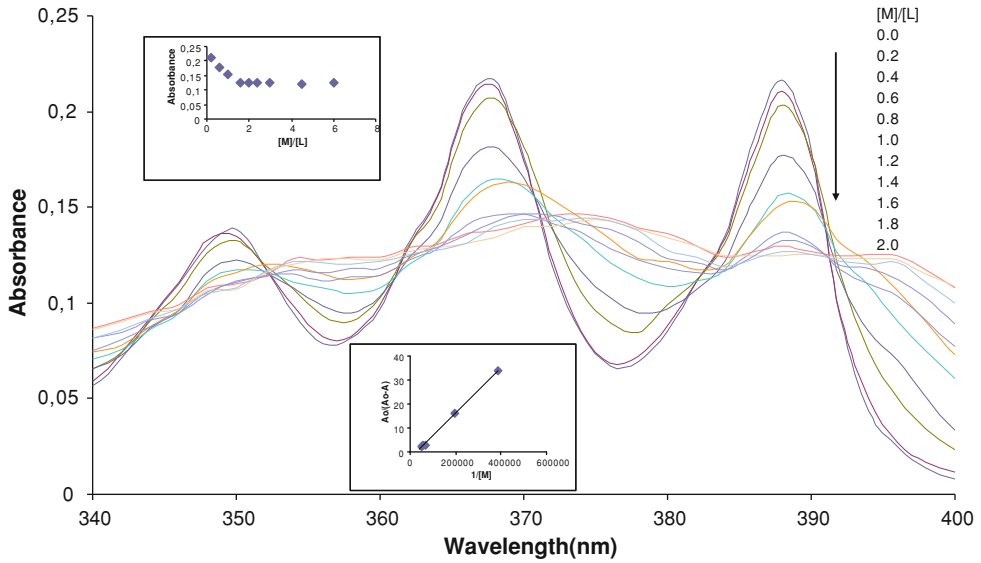

Fig. 7 The variation of the absorbance of the ligand **(3)** with the concentration of Hg^{2+}, added as 0–2 equivalents of $Hg(ClO_4)_2$. Ligand concentration = 2.58×10^{-5} M. *Insets*: Measurements were carried out at 388 nm

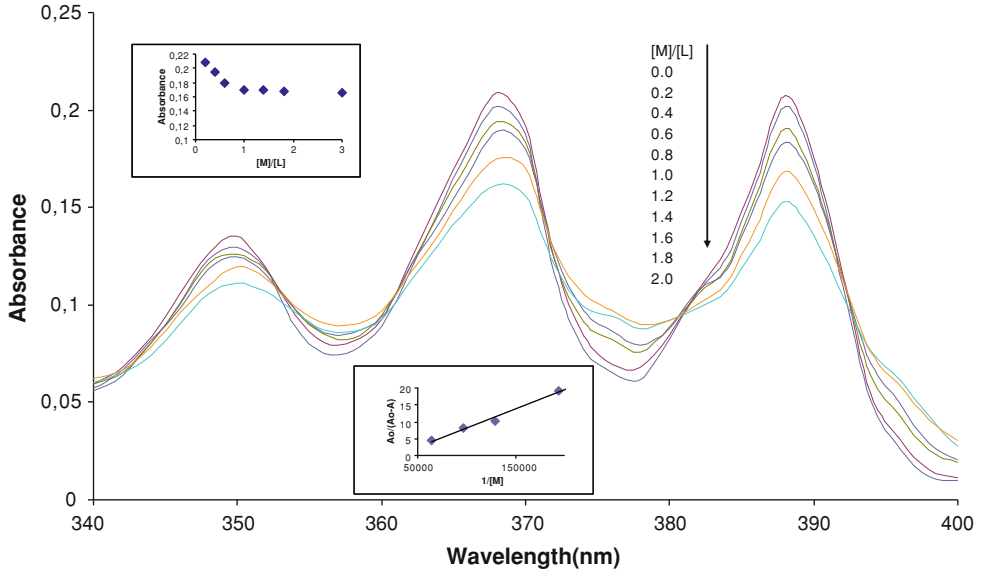

Fig. 8 The variation of the absorbance of the ligand **(3)** with the concentration of Pb^{2+}, added as 0–2 equivalents of $Pb(ClO_4)_2$. Ligand concentration = 2.58×10^{-5} M. *Insets*: Measurements were carried out at 388 nm

concentrations. However, a regular absorption decrease was observed at the 388 nm absorption band for these cations. We disclosed the formation of a stable 1:1 (M:L) complex with Zn^{2+} and Pb^{2+} from the absorbance changes both at 368 nm and at 388 nm (Figs. 8, 9 insets above). The values of Log K were 4.71 and 4.39 for Zn^{2+} and Pb^{2+}-complexes, respectively (Table 1). Figure 10 shows the effect of the increasing Al^{3+} concentration on the absorption spectra. There were three isobestic points at about 354, 373, and 393 nm. These results show that there were many species corresponding to the absorption in the solutions as similar to those of the other metal cations. The molar ratio plot is shown in Fig. 10 (inset above) where the breakpoint was 1.0, indicating that the ligand **(3)** forms a stable 1:1 (M:L) complex with Al^{3+}. Sung et al. found similar results with an anthracene-based fluorescent PET sensor [24]. On the other hand, we obtained similar results with similar 16-membered diazadithia crown ether carrying two pendant anthracene groups in a previous study. A log K value of 4.75 was found for Al^{3+} (Fig. 10 inset below).

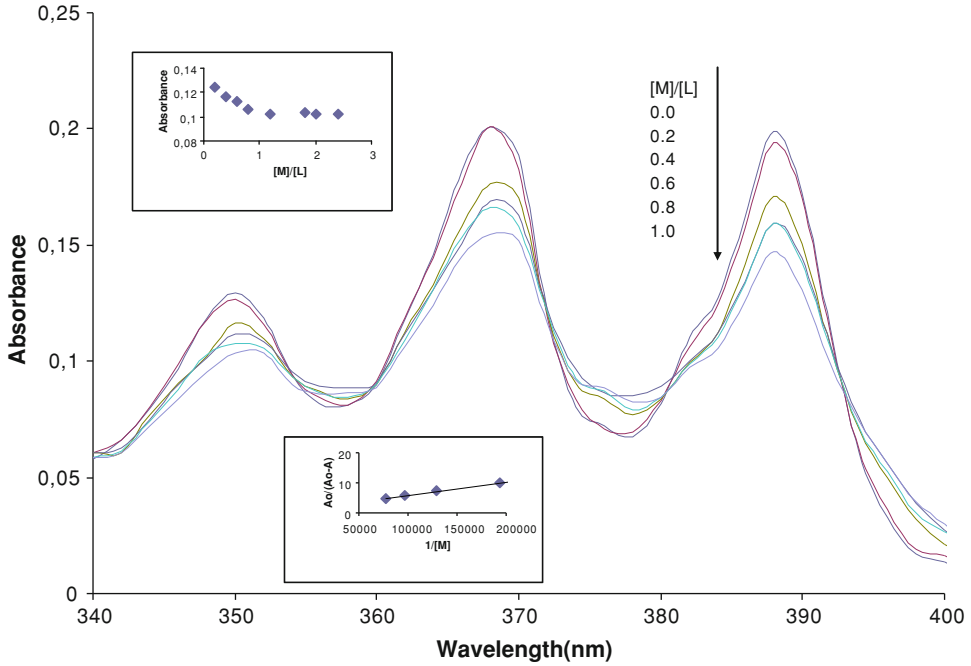

Fig. 9 The variation of the absorbance of the ligand **(3)** with the concentration of Zn^{2+}, added as 0–1 equivalent of $Zn(ClO_4)_2$. Ligand concentration = 2.58×10^{-5} M. *Insets*: Measurements were carried out at 388 nm

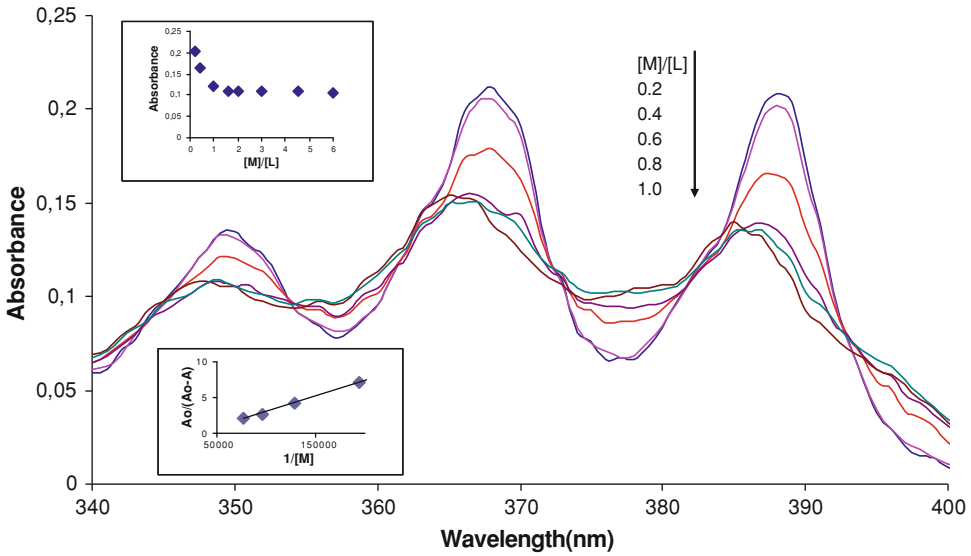

Fig. 10 The variation of the absorbance of the ligand **(3)** with the concentration of Al^{3+}, added as 0–1 equivalent of $Al(ClO_4)_3$. Ligand concentration = 2.58×10^{-5} M. *Insets*: Measurements were carried out at 388 nm

Table 1 shows the composition and the log K values of the complexes. As seen from Table 1, the most stable complex is the Cd^{2+}-ligand **(3)** complex for which the log K value is 4.79. This result can be explained with HSAB concept [25]. As known, soft metal cations prefer sulfur as donor atom during macrocyclic complexation. Therefore the stable complex may be expected between the soft Cd^{2+} cation and soft sulfur donors of the crown cavity. Then, we can see the Al^{3+}-ligand **(3)** complex with the log K value of 4.75. Actually, it is not expected to form the stable Al^{3+} complex according to HSAB concept. However, there were many factors affecting the stability of the complex in macrocyclic chemistry [26]. We can explain the complex stability of Al^{3+} with the density of charge. The high charge density of Al^{3+} causes an effective interaction between the cation and crown donor atoms. It is interesting that there was a regular increase in the stability constant with decreasing ionic diameter for the first row transition

metals, Zn^{2+}, Fe^{2+}, Fe^{3+} and Cu^{2+} hence the most stable complex belongs to Zn^{2+} with a log K value of 4.71. Ionic diameters are 1.48, 1.84, 1.53 and 1.64 Å, respectively. A similar relationship was observed for heavy metal cations such as Cd^{2+} (1.94 Å), Hg^{2+} (2.22 Å) and Pb^{2+}(2.64 Å). Increasing ionic diameter causes a decrease in the stability constant. Therefore the lowest log K value i.e. 4.39 among the tested heavy metal cations belongs to Pb^{2+} cation with the highest ionic diameter.

Fluorescence spectra

Excitation at 368 nm of the ligand **(3)** gives characteristic emission bands of anthracene between 380 and 450 nm. As seen from Fig. 1, fluorescence spectral behavior of ligand **(3)** showed a weak emission band at 415 nm (shown as c). The emission band intensity of the ligand was reduced by about 92% with respect to that of the standard substance 9-(chloromethyl) anthracene (Fig. 1, shown as b). The weak fluorescence intensity can be explained in a way that the emission of anthracene group is quenched by intramolecular photo-induced electron transfer from the lone pair of electrons of the nitrogen to the adjacent anthracene group. This result is similar to that for the classical fluorescent-azacrown system [24, 27, 28].

The fluoroionophoric properties of the ligand **(3)** were investigated by fluorescence measurements in the excess of Al^{3+}, Zn^{2+}, Fe^{2+}, Fe^{3+}, Co^{2+}, Ni^{2+}, Co^{2+}, Cd^{2+}, Hg^{2+} and Pb^{2+} ions. Figure 11 shows the effects of these metal cations on the fluorescence spectra of **(3)**. As can be seen, the emission band intensities for **(3)** are increased little by the presence of Co^{2+}, Ni^{2+} and Mn^{2+} cations. As mentioned above, these metal cations did not form any stable

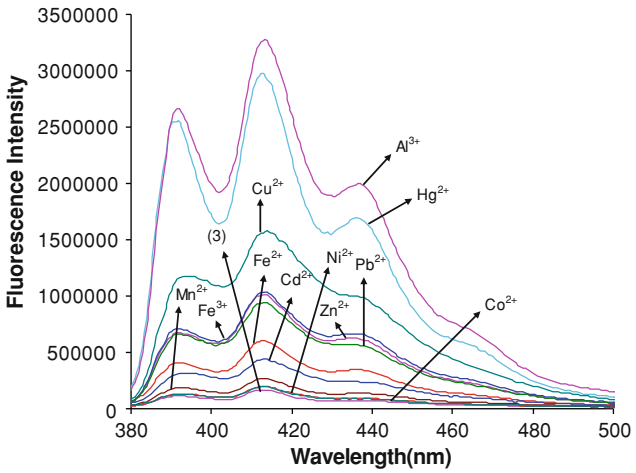

Fig. 11 Effects of metal cations on the fluorescence spectra of the ligand **(3)** in acetonitrile–dioxane (1/1). (Ligand concentration = 2.58×10^{-6} M. Metal perchlorate concentration = 2.58×10^{-5} M. Excitation at 368 nm.)

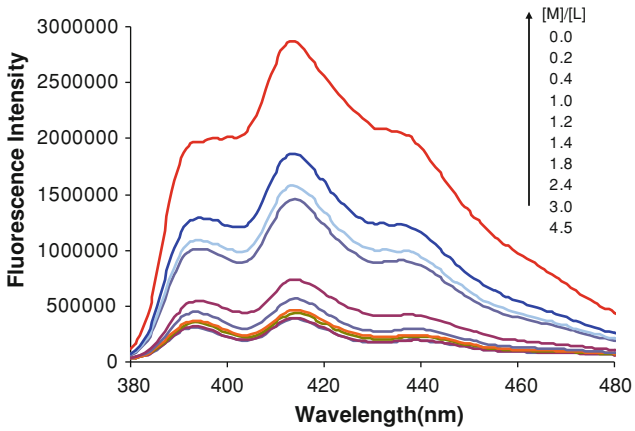

Fig. 12 The variation of the fluorescence of the ligand **(3)** with the concentration of Al^{3+} added as 0–4.5 equivalents of $Al(ClO_4)_3$. Ligand concentration = 1.3×10^{-6} M. λ_{ex} = 368 nm

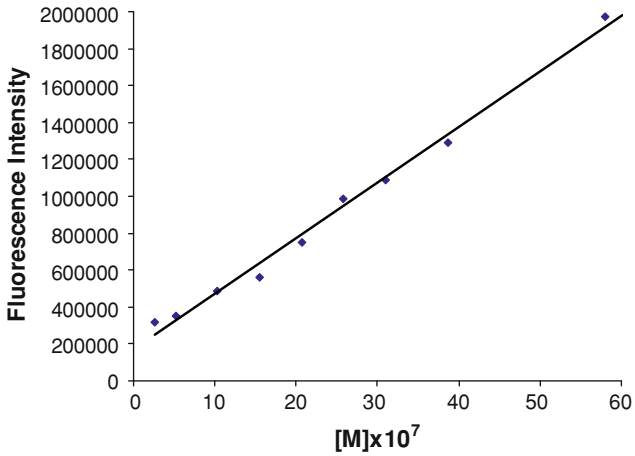

Fig. 13 Fluorescence intensity of the ligand **(3)** versus the Al^{3+} concentration for the spectrofluorimetric titration. Wavelength: 414 nm

complex with the ligand **(3)**. Zn^{2+}, Fe^{2+}, Fe^{3+}, and Pb^{2+} caused substantial increase in the emission band intensities of the ligand **(3)**. There is strong enhancement in the fluorescence emission with the transition metal cations of Cu^{2+} and Hg^{2+}. Even stronger enhancement is observed with Al^{3+}. We expected results of fluorescence enhancement for cations such as Zn^{2+}, Al^{3+}, and Cd^{2+} according to the results of spectrophotometric titration, since the complexes of these cations had high log K values with respect to those of other metal complex. As expected, fluorescence enhancements were observed in the case of these cations. The highest enhancement was observed for Al^{3+}. However, the modest fluorescence enhancement for Cd^{2+} with respect to the other complexing metal cations is interesting. Because the Cd^{2+} complex had the highest log K value of 4.79 (Table 1). These results arise from the chelation enhanced fluorescence (CHEF) in the presence of

metal cations. The complexation with metal cations hinders photoinduced electron transfer (PET) from nitrogen donor atom in crown cavity to anthryl side arm in the excited state. Therefore the loss of fluorescence via PET was prevented. Consequently, an enhancement in fluorescence intensity of the fluoroionophore is observed upon the interaction of metal cation with the nitrogen atom of crown ether cavity.

On the other hand, the regular fluorescence response was detected for Al^{3+} with the ligand **(3)**. Figure 12 shows the regular fluorescence enhancement depending on increasing Al^{3+} concentrations with **(3)**. A linear response of the fluorescence intensity at 414 nm as a function of Al^{3+} concentration was observed from 2.6×10^{-7} to 5.8×10^{-6}M with linearly dependent coefficient R^2=0.9911 (Fig. 13). The detection limit calculated as three times the standard deviation of the blank signal was found to be 6.3×10^{-8} M.

Acknowledgment This work was supported by The Scientific and Technological Research Council of Turkey (TUBITAK).

References

1. Suvadeep, N., Maitra, U.: A simple and general strategy for the design of fluorescent cation sensor beads. Org. Lett. **8**, 3239–3242 (2006)
2. Kulatilleke, C.P., Silva, S.A., Eliav, Y.: A coumarin based fluorescent photoinduced electron transfer cation sensor. Polyhedron **25**, 2593–2596 (2006)
3. Silva, S.A., Zavaleta, A., Baron, D.E., Allam, O., Isidor, E.V., Kashimura, N., Percarpio, J.M.: A fluorescent photoinduced electron transfer sensor for cations with an off-on-on-off proton switch. Tetrahedron Lett. **38**, 2237–2240 (1997)
4. Koskela, S.J.M., Fyles, T.M., James, T.D.: A ditopic fluorescent sensor for potassium fluoride. Chem. Commun., 945–947 (2005)
5. Chovelon, J.M., Grabchev, I.: A novel fluorescent sensor for metal cations and protons based of bis-1, 8-naphthalimide. Spectrochim Acta Part A **67**, 87–91 (2007)
6. Silva, A.P., Silva, S.A.: Fluorescent signalling crown ethers; "switching on" of fluorescence by alkali metal ion recognition and binding in situ. Chem. Commun., 1709–1710 (1986)
7. Kubo, K., Sakurai, T.: Syntesis and fluorescence properties of N-(1-pyrenylmethyl)-18-azacrown-6 ether. Rep. Inst. Adv. Mat **10**, 85–87 (1996)
8. Park, S.M., Kim, M.H., Choe, J.I., No, K.T., Chang, S.K.: Cyclam bearing diametrically disubstituted pyrenes as Cu^{2+}-and Hg^{2+} selective fluoroionophores. J. Org. Chem **72**, 3550–3553 (2007)
9. Kubo, K., Ishige, R., Kubo, J., Sakurai, T.: Synthesis and complexation behavior of N-(1-naphtylmethyl)-1, 4, 7, 10, 13-pentaoxa-16-azacyclooctadecane. Talanta **48**, 181–187 (1999)
10. Valeur, B., Leray, I.: Design principles of fluorescent molecular sensors for cation recognition. Coord. Chem. Rev. **205**, 3–40 (2000)
11. Maitra, U., Nath, S.: A bile acid derived potassium ion sensor. Arkivoc, 133–143 (2005)
12. Ji, H.F., Dabestani, R., Hettich, R.L., Brown, G.M.: Optical sensing of cesium using 1, 3-alternate calix[4]-mono-and di(anthrylmethyl)aza-crown-6. Photochem. Photobiol. **70**, 882–886 (1999)
13. Xu, X., Xu, H., Ji, H.F.: New fluorescent probes for the detection of mixed sodium and potassium metal ions. Chem. Commun., 2092–2093 (2001)
14. Unob, F., Asfari, Z., Vicens, J.: An anthracene-based fluorescent sensor for transition metal ion derived from calix[4]arene. Tetrahedron Lett. **39**, 2951–2954 (1998)
15. Shiraishi, Y., Kohno, Y., Hirai, T.: Bis-azamacrocyclic anthracene as a fluorescent chemosensor for cation in aqueous solution. J. Phys. Chem. B **109**, 19139–19147 (2005)
16. Silva, S.A., Kasner, M.L., Whitener, M.A., Pathirana, S.L.: A computational study of a fluorescent photoinduced electron transfer (PET) sensor for cations. J. Quan. Chem. **100**, 753–757 (2004)
17. Chang, J.H., Kim, H.J., Park, J.H., Shin, Y.K., Chung, Y.: Hluorescence intensity changes for anthrylazacrown ethers by paramegnetic metal cations. Bull. Korean Chem. Soc. **20**, 796–800 (1999)
18. Witulski, B., Weber, M., Bergstrasser, U., Desvergne, J.P., Bassani, D.M., Bouas-Laurent, H.: Novel alkali cation chemosensors based on N-9-anthrylaza-crown ethers. Org. Lett. **3**, 1467–1470 (2001)
19. Witulski, B., Zimmermann, Y., Darcos, V., Desvergne, J.P., Bassani, D.M., Bouas-Laurent, H.: N-(9-anthryl)aza-18-crown-6: palladium-catalysed synthesis, photophysical properties and cation binding ability. Tetrahedron Lett. **39**, 4807–4808 (1998)
20. Jia, L.H., Guo, X.F., Liu, Y.Y., Qian, X.H.: Anthracylmethyl benzoazacrown ether as selective fluorescence sensors for Zn^{2+}. Chin. Chem. Lett. **15**, 118–120 (2004)
21. Başoğlu, A., Parlayan, S., Ocak, M., Alp, H., Kantekin, H., Özdemir, M., Ocak, Ü.: Polyhedron **28**, 1115–1120 (2009)
22. Martin, J.W.L., Organ, G.J., Wainwright, K.P., Weerasuria, K.D.V., Willis, A.C., Wild, S.B.: Copper(I) complexes of 14- and 16-membered chelating macrocycles with trans-disposed pairs of imine-N and thioether-S donors: crystal and molecular structures of $[Cu(C_{18}H_{18}N_2S_2)]CF_3SO_3$ and $[Cu(C_{20}H_{22}N_2S_2)]CF_3SO_3$. Inorg. Chem. **26**, 2963–2968 (1997)
23. Khin, C., Lim, M.D., Tsuge, K., Iretskii, A., Wu, G., Ford, P.C.: Amine nitrosation via NO reduction of the polyamine copper(II) complex $Cu(DAC)^{2+}$. Inorg. Chem. **46**, 9323–9331 (2007)
24. Sung, K., Fu, H.K., Hong, S.H.: A Fe^{3+}/Hg^{2+}-selective anthracene-based fluorescent PET sensor with tridentate ionophore of amide/β-amino alcohol. J. Fluoresc. **17**, 383–389 (2007)
25. Evans, J. (ed.): In Supramolecular Chemistry, pp. 15–30. Oxford Universty Press Inc., New York (1999)
26. Izatt, R.M., Pawlak, K., Bradshaw, J.S., Bruening, R.L.: Thermodinamic and kinetic data for macrocycle interaction cations, anions and neutral molecules. Chem. Rev. **95**, 2529–2586 (1995)
27. Seo, H.S., Karim, M.M., Lee, S.H.: Selective fluorimetric recognition of cesium ion by 15-crown-5-anthracene. J. Fluoresc. **18**, 853–857 (2008)
28. Sing, P., Kumar, S.: Syntesis and photophysical behavior of thiaaza macrocycles with 9-anthracenylmethyl moiety as fluorescent appendage. J. Incl. Phenom. Macrocycl. Chem. **59**, 155–165 (2007)